Characterization of Mitogen-Activated Protein Kinase (MAPK) Dimers†

Julie L. Wilsbacher,‡,§ Yu-Chi Juang,‡ Andrei V. Khokhlatchev,‡,|| Ewen Gallagher,‡,⊥ Derk Binns,‡ Elizabeth J. Goldsmith,# and Melanie H. Cobb*,‡

Departments of Pharmacology and Biochemistry, University of Texas Southwestern Medical Center, 6001 Forest Park Road, Dallas, Texas 75390-9041

Received May 25, 2006; Revised Manuscript Received September 2, 2006

ABSTRACT: Phosphorylated ERK2 has an increased capacity to form homodimers relative to unphosphorylated ERK2. We have characterized the nature of the ERK2 dimer and have mutated residues in the crystal dimer interface to examine the impact of dimerization on ERK2 activity. Analysis of the mutants by gel filtration indicates that at least five residues must be mutated simultaneously to produce an ERK2 mutant that is predominantly monomeric. Mutants, whether monomers or dimers, have specific protein kinase activities under fixed assay conditions that are roughly equivalent to wild-type ERK2. The ratio of dimers to monomers is increased as the salt concentration increases, consistent with a strong hydrophobic contribution to the energy of dimer formation. ERK2 dimerization also requires divalent cations. Sedimentation analysis indicates that the related c-Jun N-terminal kinase SAPKαI/JNK2 also forms dimers, but dimerization displays no dependence on phosphorylation; the unphosphorylated and phosphorylated forms of the kinase behave similarly, with low micromolar dimer dissociation constants.

An important factor in determining the actions of mitogen-activated protein kinases (MAPKs) is their subcellular location. Stimulation of many cells by growth factors promotes the nuclear accumulation of active ERK1/2, where they phosphorylate transcription factors and other nuclear substrates (*1*−*3*). The nuclear localization of the active, phospho forms of ERK1/2 is required for some cellular programs, including mitogenesis of CCL39 fibroblast cells, serum-induced S-phase entry, neurite outgrowth in PC12 cells, and transformation of NIH3T3 cells, among others (*4*−*7*). Our earlier studies suggested that dimerization of ERK2 had an impact on its nuclear localization (*2*, *8*).

Activation of ERK2 occurs upon phosphorylation of Thr183 and Tyr185 by its upstream activators, the MAPK kinases, MEK1 and MEK2. The phosphorylations profoundly activate ERK2, causing nearly a 50 000-fold increase in k_{cat} (*9*). Conformational changes induced by dual phosphorylation also promote the formation of homodimers of phosphorylated ERK2 (ERK2-P2) (*2*). The existence of ERK2 dimers was demonstrated in vitro by equilibrium sedimentation and coimmunoprecipitation. From sedimentation, the dimer dissociation constant was estimated to be near 10 nM for phosphorylated ERK2 and 20 μM for unphosphorylated ERK2 (*2*). More recent kinetic analysis suggested a monomer−dimer equilibrium with a dissociation constant of 32 nM (*10*). Studies in cells have suggested both the absence and presence of ERK2 dimers (*2*, *11*, *12*).

In import reconstitution assays, unphosphorylated ERK2 rapidly enters and exits the nucleus facilitated by direct interactions with nucleoporins (*13*, *14*). This conclusion was supported by live-cell-imaging studies (*12*). The mechanisms controlling localization of the active, phosphorylated form remain uncertain. The requirements for the nuclear accumulation of ERK1/2 vary by cell type (*3*). In several fibroblast cell lines, ligands that activate ERK1/2 also cause their nuclear accumulation. Previously, we microinjected ERK2 and mutants into REF52 fibroblasts and followed their subcellular localization. We found that phosphorylation of ERK2 was sufficient to induce ERK2 nuclear accumulation, but its activity was dispensable (*2*). Because a monomeric mutant, H176E,L_4A ERK2, was impaired in its ability to translocate to the nucleus, we hypothesized that dimerization contributes to nuclear accumulation of ERK2, perhaps by promoting interactions with dimeric transcription factor substrates. An active transport mechanism was proposed for the dimeric form based on evidence that a β-galactosidase/*Xenopus* ERK2 fusion analogous to ERK2 H176E,L_4A was unable to be actively imported into the nucleus, whereas the wild-type ERK2 fusion was imported (*11*). Consistent with the findings using fusion proteins, recent studies using a nuclear import reconstitution system also suggested that an energy-dependent entry mechanism exists for phosphorylated ERK2 (*15*).

A 2-fold symmetric dimer observed in the crystal structure of phosphorylated ERK2 involves residues near the phosphorylation site that undergo phosphorylation-dependent

† This work was supported by grants from the National Institutes of Health (DK34128 to M.H.C. and DK46993 to E.J.G.) and the Welch Foundation (I1243 to M.H.C.). J.L.W. was supported by a predoctoral fellowship from the Howard Hughes Medical Institute.

* To whom correspondence should be addressed: Department of Pharmacology, 6001 Forest Park Rd., Dallas, TX 75390-9041. Telephone: 214-645-6122. Fax: 214-645-6124. E-mail: melanie.cobb@utsouthwestern.edu.

‡ Department of Pharmacology.

§ Present address: Abbott Laboratories, Abbott Park, IL.

|| Present address: Department of Pathology, University of Virginia, Charlottesville, VA.

⊥ Present address: Department of Immunology and Molecular Pathology, Royal Free and University College Medical School, London, U.K.

Department of Biochemistry.

10.1021/bi061041w CCC: $33.50
Published on Web 10/14/2006

conformational changes (*8*). The dimer interface consists of a nonhelical leucine zipper formed by residues in the C terminus and a network of interactions between residues in the phosphorylation lip and the C terminus (*2*). The residues in the crystal dimer were found to be protected in solution by deuterium exchange (*16*). Consistent with kinetic studies (*10*), the dimer is symmetrical and the active sites are accessible in both molecules of ERK2.

Here, we have examined the behavior of the ERK2 dimer and have probed interactions required for dimerization. Dimerization is sensitive to the salt concentration and requires divalent cations. Mutation of any single residue in the ERK2 dimer interface does not prevent dimerization, consistent with the importance of multiple contacts in the formation of dimers.

EXPERIMENTAL PROCEDURES

Generation of Mutants. ERK2 mutations were generated using the QuikChange kit (Stratagene, La Jolla, CA). Mutations were initially made in the plasmid, ERK2NpT7His$_6$ (*17*). The mutated fragments were then subcloned into wild-type or mutated forms of the bacterial coexpression system plasmid, R4FMEK1 plus ERK2pETHis$_6$ (*2*, *18*). The stress-activated protein kinase SAPKαI (*19*) also known as c-Jun N-terminal kinase (JNK2) was expressed from pRSET SAPKαI and from the bacterial coexpression system (*18*).

Purification of Proteins. His$_6$-tagged proteins were expressed and purified as described in detail previously, using coexpression in bacteria with upstream kinases for the active forms (*18*). The purest fractions of phosphorylated protein were used for further steps. Protein concentrations were determined with the Bio-Rad protein assay. As necessary, the phosphorylated ERK2 proteins were concentrated to greater than 0.4 mg/mL in a Microcon 10 concentrator (Amicon, Beverly, MA).

Gel Filtration. Proteins were dialyzed into gel-filtration buffer [12.5 mM *N*-2-hydroxyethylpiperazine-*N*′-2-ethanesulfonic acid (Hepes) at pH 7.3, 100 mM KCl, and 6.25% glycerol] containing 0.5 mM dithiothreitol (DTT). Proteins were diluted to 0.4 mg/mL in gel-filtration buffer, and 50 μL was applied to a 24 mL Superdex G75 HR 10/30 gel-filtration column equilibrated in and eluted with the same buffer. The Stokes radii of ERK2 and phosphorylated ERK2 were calculated from analytical sedimentation data (*2*). In gel-filtration experiments, the radii were estimated by comparing the elution time to the elution times of standard proteins, bovine serum albumin (BSA), ovalbumin, chymotrypsinogen, and ribonuclease A (RNase A). Apparent association constants were calculated on the basis of an eluted concentration of dimer (*C*) of the wild-type protein of 11 nM from the following equation:

$$K_A = (1 - \alpha)/4C\alpha^2$$

where α is the degree of dissociation.

Sedimentation Equilibrium. Samples were centrifuged in a Beckman XL-I analytical ultracentrifuge using an AN60Ti rotor with a six-channel, double-sector centerpiece (optical path length of 1.2 cm). The samples were centrifuged at 18 000 rpm and 4 °C until equilibrium was reached. The data were collected using absorbance optics at a wavelength of 280 nm. Samples were analyzed in a buffer of composition: 10 mM Tris at pH 7.5, 100 mM NaCl, and 0.5 mM DTT. The partial specific volume was calculated to be 0.7281 mL/g at 4 °C based on the predicted amino acid sequence using the sedimentation interpretation program (version 1.0). The solvent density was estimated to be 1.00442 g/mL at 4 °C using the same program. Data were collected on two or four concentrations of protein. Dissociation constants were determined by fitting the data collectively to a monomer/dimer equilibrium using the Beckman Optima XL-A/XL-1 data analysis software, version 4.0. Equilibrium constants from the Beckman software are in terms of absorbance units. The equilibrium constants were converted to concentration from the following formula:

$$K_{1,2}\ (\text{in units of } \text{M}^{-1}) = K_{1,2}\ (\text{in units of } \text{abs}^{-1}) \times 1.2\epsilon/2$$

where ϵ is the extinction coefficient for the protein. The extinction coefficient was calculated to be 56 380 M^{-1} at 280 nm from the amino acid composition.

Immunoblotting. Proteins in the gel-filtration fractions were separated by sodium dodecyl sulfate−polyacrylamide gel electrophoresis (SDS−PAGE), transferred to nitrocellulose, and immunoblotted with anti-ERK1/2 Y691 as described (*20*) and anti-pERK1/2 (E10, NEB) according to the protocol of the manufacturer.

Protein Kinase Assays. Activities of phosphorylated wild-type or mutant ERK2 were determined using myelin basic protein (MBP, Sigma) as the substrate. Phosphorylated ERK2 was diluted to 10 μg/mL in kinase buffer (20 mM Hepes at pH 8.0, 10 mM $MgCl_2$, 0.1 mM benzamidine, and 0.1 mM DTT). Reactions were then performed with 0.2 mM ATP (1500−8000 cpm/pmol [γ-^{32}P]ATP), 0.5 mg/mL MBP, and 200 ng/mL phosphorylated ERK2 at 30 °C for 15 min and stopped by the addition of electrophoresis sample buffer. Aliquots of reactions were analyzed by SDS−PAGE. Gels were stained with Coomassie blue and dried, and MBP bands were excised and counted by liquid scintillation.

RESULTS

The ERK2 dimer interface is formed from a nonhelical leucine zipper composed of L333, L336, and L344 from each ERK2 monomer. There are two ion pairs on each end of the interface, formed by the same two residues, H176 from the activation loop and E343 from the C terminus. These are the only ion pairs in the interface. A total of 11 residues from each monomer participate in the dimer interface (Figure 1). A total of 22 C−C interactions less than 3.8 Å were noted, and half of the close contacts (less than 3.5 Å) involved backbone contacts with side chains (Table 1). Unphosphorylated ERK2 was superimposed on the phosphorylated dimer in the N-terminal domain to highlight the conformational changes (Figure 2). A few residues that participate in the interface move significantly to form contacts in the dimer. The distances between these residues in the modeled unphosphorylated ERK2 dimer are as large as 27 Å.

To determine the effect of ERK2 residues on dimer formation, we mutated interface residues to alanine or glutamic acid to disrupt all of the contacts formed between side chains. Glutamic acid was used to introduce repulsion between the two ERK2 molecules in the dimer. The stability of ERK2 and ERK2 mutant dimers in solutions of different compositions was assessed by gel filtration. Gel filtration

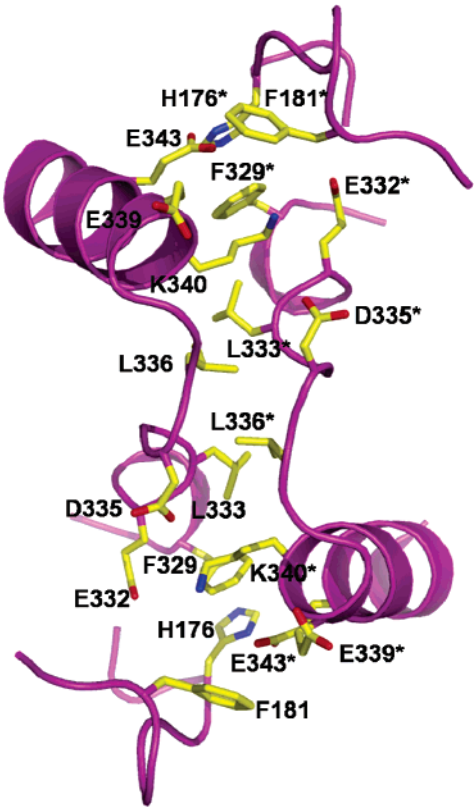

FIGURE 1: ERK2 residues that form the dimer interface. The yellow residues contribute contacts to the ERK2 dimer interface. Residue numbers are indicated. The asterisks indicate the residues contributed by the second ERK2 molecule. These residues are less that 4 Å away from each other.

Table 1: Dimer Interface Contacts

amino acid contacts[a]	contact in monomer 1[b]	contact in monomer 2[b]
E343−H176	E343 Oϵ1	H176 Nδ1
E339−F181	E339 Cγ	F181 Cζ, Cϵ2
	E339 Cβ	F181 Cζ
K340−F329	K340 Cϵ	F329 Cζ, Cϵ1
K340−E332	K340 Cδ	E332 O
K340−D335	K340 Cδ	D335 Oδ1
P337−D335	P337 Cγ, Cδ	D335 Cβ
L336−L333	L336 Cδ2	L333 O
L336−D335	L336 Cδ2	D335 O, C
D335−L336	D335 O, C	L336 Cδ2
D335−P337	D335 Cβ	P337 Cγ, Cδ
D335−K340	D335 Oδ1	K340 Cδ
L333−L336	L333 O	L336 Cδ2
E332−K340	E332 O	K340 Cδ
F329−K340	F329 Cζ, Cϵ1	K340 Cϵ
F181−E339	F181 Cζ, Cϵ2	E339 Cγ
	F181 Cζ	E339 Cβ
H176−E343	H176 Nδ1	E343 Oϵ1

[a] Residues listed are less that 4 Å from each other in the crystal structure of the phosphorylated ERK2 dimer. [b] Atoms involved in contacts are indicated. Greek letters correspond to the order of the atoms in the amino acid side chains.

was performed with phosphorylated ERK2 in 100, 250, or 500 mM KCl or NaCl. The concentration of phosphorylated ERK2 at the time of elution was approximately 22 nM. In buffer with 100 mM KCl, phosphorylated ERK2 eluted as two poorly resolved peaks (Figure 3). The first peak of phosphoERK2 corresponds to a dimer, and the second peak of phosphoERK2 corresponds to a monomer. The Stokes

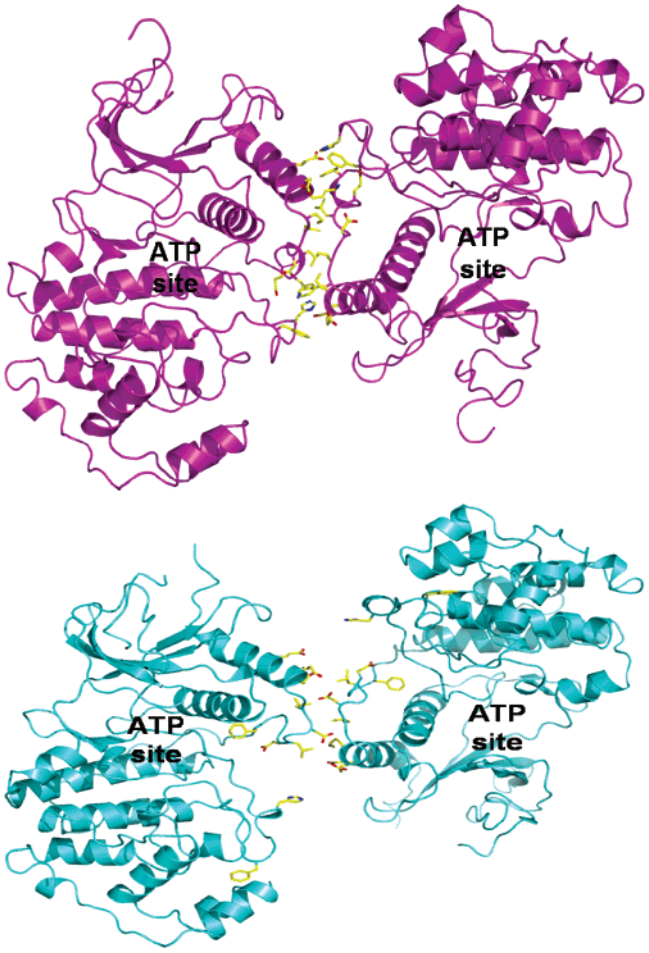

FIGURE 2: Structure of phosphorylated ERK2 and modeled unphosphorylated ERK2 dimer interface. (Top panel) Phosphorylated ERK2 dimers found in the crystal structure. Residues in the interface are yellow. (Bottom panel) PyMol (www.pymol.sourceforge.net) was used to superimpose residues of two unphosphorylated ERK2 monomers onto the coordinates of N-terminal residues of the phosphorylated ERK2 dimer crystal structure. The same interface residues are colored yellow as in the top panel.

radius of the dimer is a function of the shape, mass, and hydration of the complex; thus, it is not simply twice the Stokes radius of the monomer. Dimerized ERK2 is less hydrated because the residues in the dimer interface are not exposed to the solvent. Moreover, the shape of the dimer appears more spherical compared to monomeric ERK2. Therefore, the Stokes radii of the monomer and dimer are closer in size than might be expected on the basis of the change in molecular mass alone. The ratio of dimer to monomer is consistent with our previous estimate of the K_d of 10 nM (*2*).

Elution of phosphorylated ERK2 from the column equilibrated in 250 mM KCl resulted in an increased dimer peak height and a decreased monomer peak height, relative to the behavior in 100 mM KCl. Elution of phosphorylated ERK2 from the column equilibrated in 500 mM KCl caused a small, further increase in the dimer peak height and decrease in the monomer peak height. The increased ability of phosphorylated ERK2 to dimerize as the salt concentration is increased indicates that hydrophobic interactions are important for dimerization.

We noticed previously that co-immunoprecipitation of ERK2 dimers decreased if solutions contained chelating

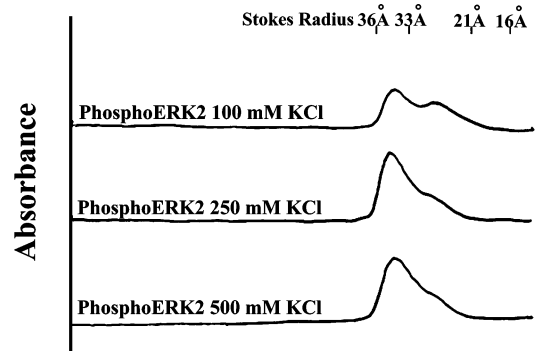

FIGURE 3: Dimerization of phosphorylated ERK2 increases as the salt concentration increases. Phosphorylated ERK2 was applied to a 24 mL Superdex G75 gel-filtration column that was equilibrated with gel-filtration buffer containing 100 mM (top), 250 mM (middle), or 500 mM (bottom) KCl. Phosphorylated ERK2 was at a concentration of approximately 22 nM at the time of elution. The *y* axis indicates the absorbance at 280 nm. Tick marks indicate Stokes radii of the standards: BSA (36 Å, 67 kDa), ovalbumin (33 Å, 43 kDa), chymotrypsinogen (21 Å, 25 kDa), and RNase A (16 Å, 13.7 kDa). The peak eluting at a Stokes radius of 35 Å corresponds to a dimer, and the peak at 27 Å corresponds to a monomer.

agents. Thus, we examined the effect of the chelating agents, ethylenediaminetetraacetic acid (EDTA) and ethylene glycol bis(2-aminoethyl ether)-*N*,*N*,*N*′,*N*′-tetraacetic acid (EGTA), on the dimerization of phosphorylated ERK2. ERK2 failed to dimerize in the presence of either agent (Figure 4), indicating that dimerization is dependent upon divalent cations. The addition of either $MgCl_2$ or $CaCl_2$ partially restored the ability of the protein to dimerize (data not shown).

A total of 10 of the phosphorylated ERK2 mutants retained the ability to dimerize significantly in 100 mM KCl (Table 2). Three mutants, delta4, delta4,L_4A, and H176E,L_4A, were almost completely monomers under these conditions. Only delta4 showed a small fraction of dimer, suggesting that a K_d for dimerization shifted by approximately 50-fold (0.5 μM). Figure 5 shows representative traces for phosphorylated wild-type ERK2, the monomeric mutant, H176E,L_4A, and the dimeric mutant, H176E,L_2E,E343A. Because H176E,L_4A was monomeric, we tested the individual contributions of H176 and the leucine zipper residues. As seen in Table 2, both of these proteins, ERK2 H176E and ERK2 L_4A (Figure 6A), persisted as dimers; the difference in the dimer/monomer ratio suggests a change in K_d for ERK2 L_4A of 5−10-fold (71 nM), the only change greater than 3-fold among all of the mutants that were primarily dimers. The mutant H176A,F181A,L_4A was also a dimer (Table 2 and Figure 6B), indicating that the introduction of charge repulsion at H176 was required to disrupt dimerization. All of the dimeric mutants showed an increase in dimerization in 500 mM KCl (Table 3). Phosphorylated ERK2 H176E,L_4A forms little or no dimer in 100 mM KCl (middle trace in Figure 7). In buffers with 100 mM NaCl, dimerization of this mutant could be detected (data not shown), and in 500 mM KCl, its behavior was similar to the wild-type protein (Table 3). Even more dramatically than for wild-type ERK2, the amount of phosphorylated ERK2 H176E,L_4A dimer increased as the salt concentration increased (Figure 7). Mutant ERK2 proteins were then tested for the ability to dimerize in the presence of EDTA. Similar to wild-type

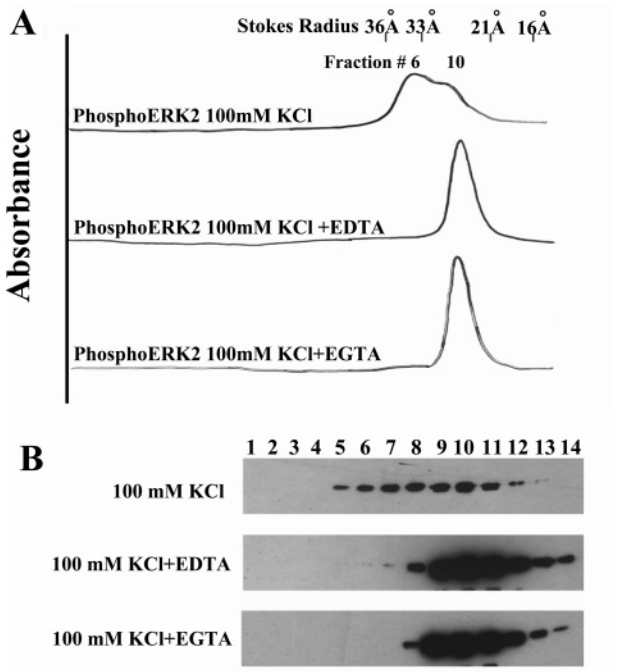

FIGURE 4: Chelating agents prevent dimerization of phosphorylated ERK2. (A) Phosphorylated ERK2 was applied to a Superdex G75 gel-filtration column that was equilibrated with gel-filtration buffer containing 100 mM KCl (top), 100 mM KCl plus 1 mM EDTA (middle), or 100 mM KCl plus 1 mM EGTA (bottom). Data are plotted as in Figure 3. (B) Samples of peak fractions from the gel-filtration elution were separated by SDS−PAGE and transferred to nitrocellulose. Blots were probed with an antibody that recognizes only the phosphorylated form of ERK1/2 (E10, NEB). The blots correspond to the gel-filtration traces shown in A: PhosphoERK2 in 100 mM KCl buffer (top), phosphoERK2 in 100 mM KCl plus 1 mM EDTA buffer (middle), and phosphoERK2 in 100 mM KCl plus 1 mM EGTA buffer (bottom).

Table 2: Dimerization of Phosphorylated ERK2 Mutants as Assessed by Gel Filtration

ERK2 mutant	residues mutated	ratio dimer/monomer[a]
wild type	none	1.6:1
delta4	deleted P174, D175, H176, and D177	0.1:1
delta4, L_4A	deleted 174−177, L333, L336, L341, L344	0:1
H176E	H176	0.8:1
L_2E	L333, L336	1:0
L_4A	L333, L336, L341, L344	0.44:1
H176E, E343A	H176, E343	1.1:1
H176E, L_4A	H176, L333, L336, L341, L344	0:1
H176E, L_2E, E343A	H176, L333, L336, E343	1.6:1
H176A, F181A, L_4A	H176, F181, L333, L336, L341, L344	0.8:1
F329A	F329	2.4:1
E339A	E339	dimer
K340A	K340	1:0
K340E, L_3E	K340, L333, L336, L344	1.48:1

[a] Phosphorylated ERK2 and mutants were tested for dimerization by gel filtration as indicated in the caption of Figure 3. The ratios of the absorbance at 280 nm of the monomer and dimer peaks are indicated.

ERK2, all of the mutants tested eluted as monomers in buffer with EDTA (Table 3).

Finally, we tested the effect of dimerization on ERK2 activity. The ERK2 structures that are involved in dimer-

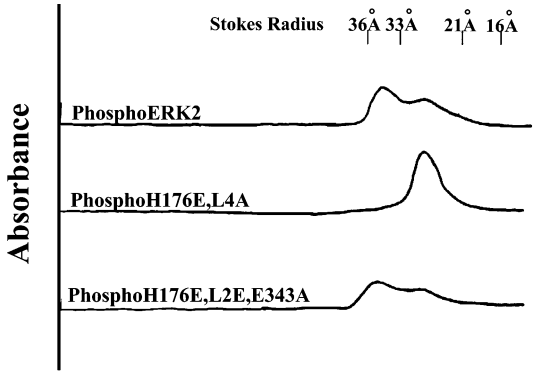

FIGURE 5: Gel filtration of ERK2 and ERK2 mutants. Phosphorylated ERK2 (top), H176E,L_4A (middle), and H176E,L_2E,E343A (bottom) were applied to a Superdex G75 gel-filtration column that was equilibrated with 100 mM KCl gel-filtration buffer. Tick marks indicate Stokes radii of the standards as in Figure 3.

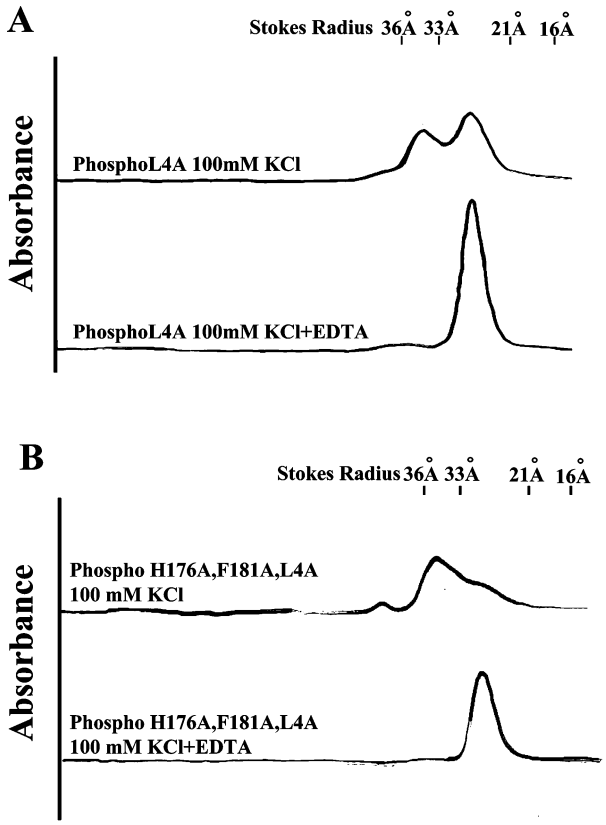

FIGURE 6: Gel filtration of ERK2 L_4A and ERK2 H176A, F181A, L_4A. (A) Phosphorylated L_4A was applied to a Superdex G75 gel-filtration column that was equilibrated with 100 mM KCl gel-filtration buffer (top) or 100 mM KCl plus 1 mM EDTA gel-filtration buffer. (B) Phosphorylated H176A, F181A, L_4A was applied to a Superdex G75 gel-filtration column that was equilibrated with 100 mM KCl gel-filtration buffer (top) or 100 mM KCl plus 1 mM EDTA gel-filtration buffer (bottom). Tick marks indicate Stokes radii of the standards as in Figure 3.

ization are also those that propagate the conformational changes that activate the kinase; thus, dimerization might stabilize or otherwise alter kinase activity. The specific activities of wild-type and mutant phosphorylated ERK2 proteins were tested against a monomeric substrate, MBP, in an in vitro kinase assay. The mutants had specific activities toward MBP that were no more than 2-fold different from that of wild-type ERK2 (Figure 8).

Table 3: Dimerization of Phosphorylated ERK2 Mutants as Assessed by Gel Filtration in Different Buffers

ERK2 mutant	500 mM salt buffer[a] dimer/monomer ratio	100 mM salt and 1 mM EDTA buffer[a]
wild type	2.25:1	monomer
delta4	ND	ND
delta4, L_4A	ND	ND
H176E	2.09:1	monomer
L_2E	1.2:1	monomer
L_4A	1.5:1	monomer
H176E, E343A	1:0	monomer
H176E, L_4A	3.8:1	monomer
H176E, L_2E, E343A	3.3:1	monomer
H176A, F181A, L_4A	1.8:1	monomer
F329A	5.1:1	monomer
E339A	ND	ND
K340A	0.6:1	monomer
K340E, L_3E	1.75:1	monomer

[a] Phosphorylated ERK2 and mutants were tested for dimerization by gel filtration as indicated in the caption of Figure 3. Ratios were determined as in Table 2.

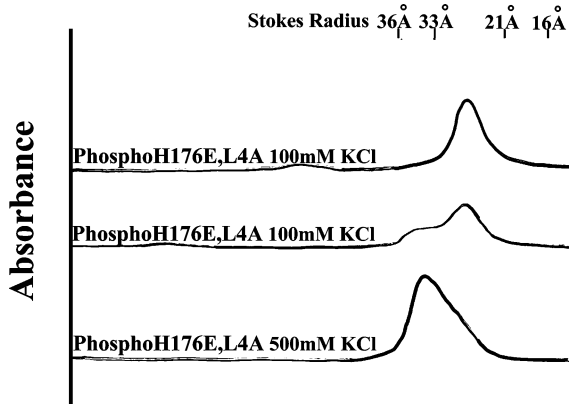

FIGURE 7: Dimerization of phosphorylated ERK2 H176E,L_4A increases over time and as the salt concentration increases. Phosphorylated ERK2 H176E,L_4A was applied to a Superdex G75 gel-filtration column that was equilibrated with gel-filtration buffer containing 100 mM (top and middle) or 500 mM (bottom) KCl. The middle trace was obtained from a gel filtration performed 5 h after the top trace. Data are plotted as in Figure 3.

Crystal structures of other unphosphorylated or phosphorylated MAPKs have not provided any evidence for dimers (*21*−*24*). Preliminary sedimentation experiments with p38α suggested that it did form dimers but at higher concentrations than ERK2 (*2*). To determine if other MAPK family members form dimers, we analyzed unphosphorylated and phosphorylated forms of SAPKαI/JNK2 using sedimentation equilibrium. Data obtained from SAPKαI/JNK2 best fit a monomer−dimer equilibrium, with a dissociation constant of ∼4.6 μM (Figure 9A). Data obtained from phosphorylated SAPKαI/JNK2 also best fit a monomer−dimer equilibrium with a dissociation constant of 2.5 μM (Figure 9B). These findings demonstrate that SAPKαI/JNK2 can form dimers but reveal little effect of phosphorylation on this behavior. An alignment of the residues forming contacts in the ERK2 dimer with the comparable residues in SAPKαI/JNK2 (Figure 9C) shows that these regions of the two molecules are poorly conserved. The overall identity between these two proteins is ∼40%. Of the 11 residues making contacts in the dimer interface (underlined residues in ERK2), only 2, E332 and E343, are identical in SAPKαI/JNK2. The sequence ^{333}LDDLP^{337} that forms the core of the dimer

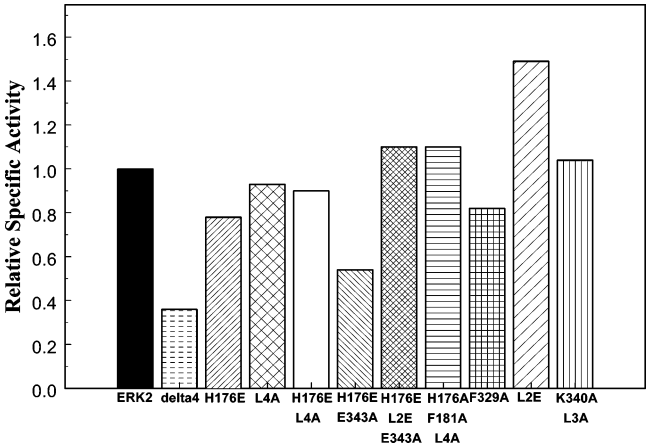

FIGURE 8: Kinase activity of phosphorylated wild-type and mutant ERK2 proteins. The kinase activity of phosphorylated ERK2 proteins was measured in an in vitro kinase assay as described in the Experimental Procedures. Data are expressed as specific activity relative to wild-type phosphorylated ERK2 included in each assay (set to 1). Shown are the representative data from one to three experiments performed for each mutant. The range of ERK2 specific activity was 0.5−2.2 μmol min^{-1} mg^{-1}.

interaction in ERK2 is replaced by the sequence EREHA in SAPKαI/JNK2. The activation loop of SAPKαI/JNK2 has four fewer residues than that of ERK2, and there is no residue homologous to H176, which forms ion pairs at both ends of the interface in the ERK2 dimer. Thus, it is unclear from the sequences and structures of ERK2 and SAPKαI/JNK2 whether the SAPKαI/JNK2 dimer will be similar to that of ERK2.

DISCUSSION

The major goal of this study was to characterize properties of ERK2 dimers. The phosphorylated ERK2 structure reveals that the dimer interface is formed by hydrophobic as well as electrostatic interactions. No single mutation disrupted dimerization. Instead, mutations of hydrophobic residues as well as a charge repulsion were required to interfere with ERK2 dimerization. Deletion of residues from the activation loop prevents interactions of this structure with L16, destabilizing the dimer interface. The importance of charge repulsion in place of the ion pair in disrupting dimerization is further suggested by the observation that the mutation of E343, in the ion pair with H176, to alanine resulted in dimerization of the ERK2 mutant H176E, L_2E, E343A.

Dimerization is strongly dependent upon hydrophobic interactions. This was revealed most clearly by the fact that increasing ionic strength promoted dimerization. ERK2 H176E,L_4A is converted to a dimer as the ionic strength increases. This indicates that mutating these residues does not completely prevent dimerization, although changes in K_d may, nevertheless, be quite large. In addition, even in 100 mM KCl, some dimers are formed over time. Because 100 mM KCl is closest to the cellular ionic concentration, most of the studies were performed under this condition.

The relative amounts of ERK1 and ERK2 may vary by more than 10-fold in different cell types. Intracellular concentrations of ERK2 have been estimated between 50 nM to a high in excess of 1 mM in frog oocytes (*25*, *26*). Given this probable range of concentrations, it seems quite plausible that phosphorylated ERK2 will form dimers in cells, while dimerization of a significant amount of unphosphorylated ERK2 seems less likely. We originally found that H176E,L_4A ERK2 did not accumulate in the nuclei of cells after phosphorylation in the same manner as wild-type ERK2 (*2*). We have analyzed the import of this mutant in reconstitution assays and found that it enters the nucleus readily through the carrier- and energy-independent mechanism (*27*). Thus, its failure to accumulate in the nucleus to an extent equivalent to the wild type may reflect decreased binding interactions in that compartment, as previously suggested (*2*), or perhaps an impairment in a recently identified energy-dependent import mechanism for phosphorylated ERK2 (*15*), as previously implied by examination of a fusion protein (*11*). The potential functional defects in this mutant with respect to localization and substrate specificity remain to be determined.

One model for the protein−protein interaction is based on the extensive mutagenesis work of Wells and co-workers. As is seen with the binding of human growth hormone to its receptor at site 1, there may be a "hot spot" in which a few, usually hydrophobic residues are responsible for the majority of the binding energy (*28*, *29*). However, this model does not apply well to the ERK2 dimer interface, because multiple, spatially segregated mutations are required to produce a monomeric form of ERK2. Therefore, the ERK2 dimer interface does not appear to have a hot spot, or the hot spot has not been identified by the mutant combinations tested thus far.

Although there was no cation detected in the dimer interface of the phosphoERK2 crystal structure (*8*), chelating agents completely blocked dimerization. We do not know which divalent cation is required for dimerization of phosphorylated ERK2. Add back experiments suggest that both magnesium and calcium can restore dimerization. It seems likely that the cation requirement is actually due to the magnesium ion in the ATP-binding site, which may be required for an overall conformational change that is important for dimerization. However, ATP itself apparently was not necessary for the formation of dimers.

Dimerization has little effect on the specific kinase activity toward monomeric substrates under near-saturating conditions. This is consistent with previous studies, which noted no effect of the concentration on ERK2 activity (*17*). More detailed kinetic analyses suggested small differences in kinetic properties not noted here. It seems likely that dimerization will affect activity toward dimeric substrates not tested in this study.

We also wanted to determine if dimerization is unique to ERK2. The strongest biological data that could be interpreted to suggest that other MAPKs dimerize comes from work by Karin's group. They examined phosphorylation by SAPK/JNK of Jun species within Jun heterodimers. Some Jun variants contain a delta domain, a SAPK/JNK-selective targeting domain, that increases the affinity of the kinase for the substrate (*30*). They demonstrated that the association of SAPK/JNK with the delta domain of a Jun isoform that lacks its own phosphorylation sites leads to the phosphorylation of its heterodimeric partner, even if the partner lacks a delta domain. The residues involved in the ERK2 dimer interface, however, are not highly conserved among other MAPK family members (see Figure 9C), and the activation

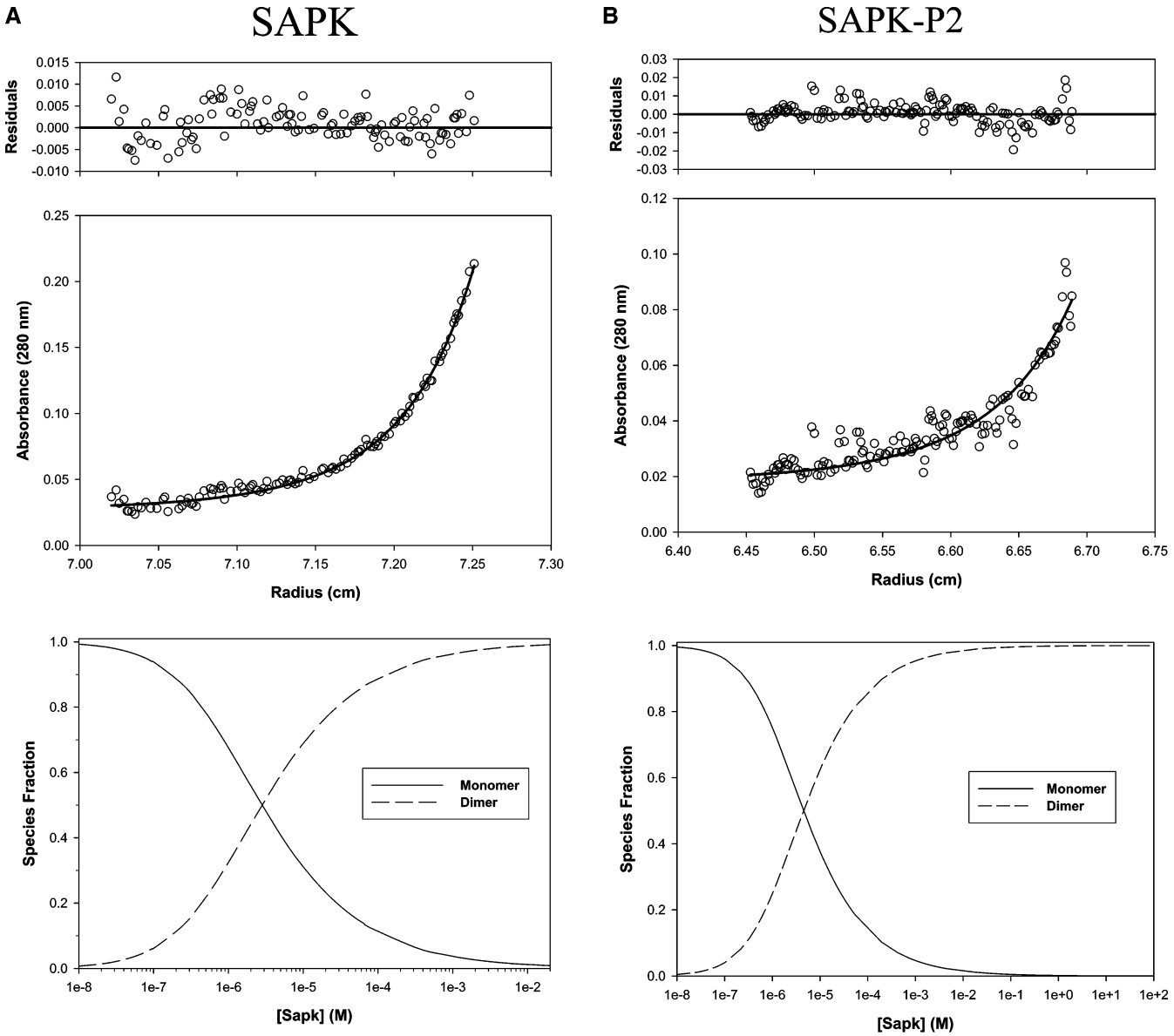

C

ERK2 ^{171}V**A**DPD_H_DHTG_F_L**T**E**YV**A**TR**^{189} ^{328}K_F_DM**E**_L_DD_LP_K**E**_K_L**K**_E_**L**^{344}

SAPK T**A**CTN FMM**T**P**YV**V**TR** DAQL**E**EREHAI**E**EW**KEL**

FIGURE 9: Equilibrium sedimentation of SAPKαI/JNK2. SAPKαI/JNK2 was centrifuged in a Beckman XL-I analytical ultracentrifuge at 18 000 rpm and 4 °C until equilibrium was reached. The data were collected using absorbance optics at a wavelength of 280 nm and analyzed using Optima data analysis software. (A) Unphosphorylated protein. (B) Phosphorylated protein. (C) Alignment of residues in SAPKαI/JNK2 with those in ERK2 that form the dimer interface.

loop, which is extended in its interaction with L16, is four to six residues shorter in SAPK/JNK and p38 family members. These differences suggest that dimerization may not be common to the family. More complete analysis of SAPKαI/JNK2 also indicated phosphorylation-independent dimerization at micromolar concentrations. The physiological relevance of its dimerization is unclear; its cellular concentrations have been estimated to be less than 10% of the dimerization K_d concentration (*31*). In view of the crystallographic and biochemical data on MAPKs and the sedimentation analysis of SAPKαI/JNK2, it seems increasingly probable that phosphorylation-induced dimerization may only occur with ERK1 and ERK2 and not with other MAPK family members.

ACKNOWLEDGMENTS

We thank Tara Beers Gibson, Bing-e Xu, and Mahesh Karandikar for critical suggestions and comments about the manuscript, Joseph P. Albanesi (UT Southwestern) for analysis of effects of mutations on relative dissociation constants of ERK2 mutants, and Dionne Ware for administrative assistance.

REFERENCES

1. Chen, R.-H., Sarnecki, C., and Blenis, J. (1992) Nuclear localization and regulation of *erk*- and *rsk*-encoded protein kinases, *Mol. Cell. Biol. 12*, 915−927.
2. Khokhlatchev, A., Canagarajah, B., Wilsbacher, J. L., Robinson, M., Atkinson, M., Goldsmith, E., and Cobb, M. H. (1998)

Phosphorylation of the MAP kinase ERK2 promotes its homodimerization and nuclear translocation, *Cell 93*, 605−615.
3. Whitehurst, A. W., Cobb, M. H., and White, M. A. (2004) Stimulus-coupled spatial restriction of extracellular signal-regulated kinase 1/2 activity contributes to the specificity of signal-response pathways, *Mol. Cell. Biol. 24*, 10145−10150.
4. Lenormand, P., Sardet, C., Pages, G., L'Allemain, G., Brunet, A., and Pouysségur, J. (1993) Growth factors induce nuclear translocation of MAP kinases ($p42^{mapk}$) but not of their activator MAP kinase kinase ($p45^{mapkk}$) in fibroblasts, *J. Cell Biol. 122*, 1079−1088.
5. Gotoh, I., Fukuda, M., Adachi, M., and Nishida, E. (1999) Control of the cell morphology and the S phase entry by mitogen-activated protein kinase kinase. A regulatory role of its N-terminal region, *J. Biol. Chem. 274*, 11874−11880.
6. Robinson, M. J., Stippec, S. A., Goldsmith, E., White, M. A., and Cobb, M. H. (1998) Constitutively active ERK2 MAP kinase is sufficient for neurite outgrowth and cell transformation when targeted to the nucleus, *Curr. Biol. 8*, 1141−1150.
7. Brunet, A., Roux, D., Lenormand, P., Dowd, S., Keyse, S., and Pouyssegur, J. (1999) Nuclear translocation of p42/p44 mitogen-activated protein kinase is required for growth factor-induced gene expression and cell cycle entry, *EMBO J. 18*, 664−674.
8. Canagarajah, B. J., Khokhlatchev, A., Cobb, M. H., and Goldsmith, E. (1997) Activation mechanism of the MAP kinase ERK2 by dual phosphorylation, *Cell 90*, 859−869.
9. Prowse, C. N., Hagopian, J. C., Cobb, M. H., Ahn, N. G., and Lew, J. (2000) Catalytic reaction pathway for the mitogen-activated protein kinase ERK2, *Biochemistry 39*, 6258−6266.
10. Waas, W. F., Rainey, M. A., Szafranska, A. E., and Dalby, K. N. (2003) Two rate-limiting steps in the kinetic mechanism of the serine/threonine specific protein kinase ERK2: A case of fast phosphorylation followed by fast product release, *Biochemistry 42*, 12273−12286.
11. Adachi, M., Fukuda, M., and Nishida, E. (1999) Two co-existing mechanisms for nuclear import of MAP kinase: Passive diffusion of a monomer and active transport of a dimer, *EMBO J. 18*, 5347−5358.
12. Burack, W. R., and Shaw, A. S. (2005) Live cell imaging of ERK and MEK: Simple binding equilibrium can explain ERK's regulated nucleocytoplasmic distribution, *J. Biol. Chem. 280*, 3832−3837.
13. Whitehurst, A. W., Wilsbacher, J. L., You, Y., Luby-Phelps, K., Moore, M. S., and Cobb, M. H. (2002) ERK2 enters the nucleus by a carrier-independent mechanism, *Proc. Natl. Acad. Sci. U.S.A. 99*, 7496−7501.
14. Matsubayashi, Y., Fukuda, M., and Nishida, E. (2001) Evidence for existence of a nuclear pore complex-mediated, cytosol-independent pathway of nuclear translocation of ERK MAP kinase in permeabilized cells, *J. Biol. Chem. 276*, 41755−41760.
15. Ranganathan, A., Yazicioglu, M. N., and Cobb, M. H. (2006) The nuclear localization of ERK2 occurs by mechanisms both independent of and dependent on energy, *J. Biol. Chem. 281*, in press.
16. Hoofnagle, A. N., Resing, K. A., Goldsmith, E. J., and Ahn, N. G. (2001) Changes in protein conformational mobility upon activation of extracellular regulated protein kinase-2 as detected by hydrogen exchange, *Proc. Natl. Acad. Sci. U.S.A. 98*, 956−961.
17. Robbins, D. J., Zhen, E., Owaki, H., Vanderbilt, C., Ebert, D., Geppert, T. D., and Cobb, M. H. (1993) Regulation and properties of extracellular signal-regulated protein kinases 1 and 2 *in vitro*, *J. Biol. Chem. 268*, 5097−5106.
18. Khokhlatchev, A., Xu, S., English, J., Wu, P., Schaefer, E., and Cobb, M. H. (1997) Reconstitution of mitogen-activated protein kinase phosphorylation cascades in bacteria, *J. Biol. Chem. 272*, 11057−11062.
19. Kyriakis, J. M., Banerjee, P., Nikolakaki, E., Dai, T., Rubie, E. A., Ahmad, M. F., Avruch, J., and Woodgett, J. R. (1994) The stress-activated protein kinase subfamily of c-Jun kinases, *Nature 369*, 156−160.
20. Boulton, T. G., and Cobb, M. H. (1991) Identification of multiple extracellular signal-regulated kinases (ERKs) with antipeptide antibodies, *Cell Regul. 2*, 357−371.
21. Wang, Z., Harkins, P. C., Ulevitch, R. J., Han, J., Cobb, M. H., and Goldsmith, E. J. (1997) The structure of mitogen-activated protein kinase p38 at 2.1-Å resolution, *Proc. Natl. Acad. Sci. U.S.A. 94*, 2327−2332.
22. Chang, C. I., Xu, B., Akella, R., Cobb, M. H., and Goldsmith, E. J. (2002) Crystal structures of MAP kinase p38 complexed to the docking sites on its nuclear substrate MEF2A and activator MKK3b, *Mol. Cell 9*, 1241−1249.
23. Bellon, S., Fitzgibbon, M. J., Fox, T., Hsiao, H. M., and Wilson, K. P. (1999) The structure of phosphorylated p38γ is monomeric and reveals a conserved activation-loop conformation, *Struct. Fold. Des. 7*, 1057−1065.
24. Xie, X., Gu, Y., Fox, T., Coll, J. T., Fleming, M. A., Markland, W., Caron, P. R., Wilson, K. P., and Su, M. S. (1998) Crystal structure of JNK3: A kinase implicated in neuronal apoptosis, *Structure 6*, 983−991.
25. Chen, Z., Gibson, T. B., Robinson, F., Silvestro, L., Pearson, G., Xu, B., Wright, A., Vanderbilt, C., and Cobb, M. H. (2001) MAP kinases, *Chem. Rev. 101*, 2449−2476.
26. Huang, C.-Y. F., and Ferrell, J. E., Jr. (1996) Ultrasensitivity in the mitogen-activated protein kinase cascade, *Proc. Natl. Acad. Sci. U.S.A. 93*, 10078−10083.
27. Whitehurst, A. W., Robinson, F. L., Moore, M. S., and Cobb, M. H. (2004) The death effector domain protein PEA-15 prevents nuclear entry of ERK2 by inhibiting required interactions, *J Biol. Chem. 279*, 12840−12847.
28. Clackson, T., and Wells, J. A. (1995) A hot spot of binding energy in a hormone-receptor interface, *Science 267*, 383−386.
29. Wells, J. A. (1996) Binding in the growth hormone receptor complex, *Proc. Natl. Acad. Sci. U.S.A. 93*, 1−6.
30. Kallunki, T., Su, B., Tsigelny, I., Sluss, H. K., Dérijard, B., Moore, G., Davis, R., and Karin, M. (1994) JNK2 contains a specificity-determining region responsible for efficient c-Jun binding and phosphorylation, *Genes Dev. 8*, 2996−3007.
31. Minden, A., Lin, A., Claret, F.-X., Abo, A., and Karin, M. (1995) Selective activation of the JNK signaling cascade and c-Jun transcriptional activity by the small GTPases Rac and Cdc42Hs, *Cell 81*, 1147−1157.

BI061041W